Rac1 signaling–associated genes are upregulated in nodal metastasis of canine oral mucosal melanoma

Rac1 signaling-associated genes are upregulated in nodal metastasis of canine oral mucosal melanoma

Stefano Di Palma, Ilaria Porcellato, Camilla Capaccia, Gabriella Guelfi, Adriana Lo Giudice, Chiara Brachelente, Willie Bergmann, Barbara Brunetti, Mike Starkey

ABSTRACT

Oral mucosal melanomas (OMMs) are the most frequent oral malignancy in dogs, characterized by aggressive local behavior and high metastatic rate. The mechanisms that drive canine OMM metastasis are still largely unknown, providing for limited therapeutic approaches once the disease has spread to metastatic sites.

The objective of this investigation was to evaluate the differences in gene expression between canine primary OMMs and their matched nodal metastases.

Transcriptional profiling of formalin-fixed, paraffin-embedded biopsies of four canine OMMs and their respective lymph node biopsies was performed using exon microarrays. Confirmation of the differential expression of selected genes was subsequently sought by quantitative RT-PCR (RT-qPCR) on 13 paired samples (primary tumor-metastatic lymph node). Results highlight the activation of pathways associated with actin cytoskeleton organization, cellular motility and migration. In particular, microarray assay indicated increased expression, in lymph node metastases, of genes (including ELMO1, VAV3 and DOCK2) associated with Rac1 signaling-regulated cell migration. The differential expression of several genes was validated by RT-qPCR.

Overall, the results of this investigation point to a significant role for Rac1 signaling in the pathogenesis of OMM metastasis to regional lymph nodes. The Rac1 signaling-associated genes highlighted herein are indeed involved in the activation of cellular migration and one, or more, may represent a future therapeutic target to prevent OMM-metastatic dissemination.

Keywords: canine oral mucosal melanoma; gene expression profiling; exon microarray; RT-qPCR; Rac1, GTP binding protein; nodal metastasis.

INTRODUCTION

Oral melanocytic tumors are common in dogs, accounting for up to 17% of all oral neoplasms[43] and approximately 30-40% of all oral malignancies.[60] In general, canine oral malignant melanomas (OMMs) are characterized by aggressive biologic behavior and shorter median survival time, when compared to their cutaneous counterpart. For dogs treated with surgery alone, the survival rate is less than 35%, and local recurrence is frequent (about 10% of cases) even when surgical margins are clean.[3] Metastases to regional lymph nodes and distant organs are frequently reported (in up to 74% of cases).[45] Tissue invasion and metastasis are biological hallmarks of malignant tumors. Metastasis is defined by the spread of neoplastic cells to sites physically discontinuous with the primary tumor. Tumor cells can reach these sites by penetrating blood vessels, lymphatics, and body cavities.

In general, metastatic dissemination appears to be facilitated by pro-metastatic genetic and epigenetic changes in the genome of the primary tumor, and interactions between neoplastic cells and other cells (such as immune cells, fibroblasts, and endothelial cells) in both the initial and distant microenvironments.[15]

The identification of pro-metastatic genetic and epigenetic events, in addition to those driving tumor development, and understanding of the pathways underpinning the metastatic cascade in cancer, is critical to discover molecular targets for the prevention and treatment of distant metastases.[5,66] In melanomas, neoplastic cells display plasticity and highly migratory behavior, facilitating dissemination to distant sites; these characteristics are likely attributed to a neural crest-like reprogramming of neoplastic

melanocytes.[25] Indeed, malignant melanoma cells reactivate pro-migratory and pro-invasive pathways, leading to aberrant dissemination.[24] Nevertheless, the pathomechanisms involved in local invasion and metastasis of both human and canine mucosal melanoma remain poorly understood.[5,6]

Recently, gene expression profiling has proven to be a powerful tool for the identification of genes involved in metastasis in canine OMM.[5] It was shown that primary OMMs that metastasized were characterized by reduced expression of CXCL12, a protein that normally stimulates the migration and activation of hematopoietic progenitor cells, endothelial cells, and several leukocytes,[10] and increased expression of APOBEC3A, when compared to non-metastasizing primary OMMs. Similarly, in human head/neck melanomas APOBEC3A overexpression has been identified, supporting its role in the increase of mutational load, and in promoting inter- and intratumoral heterogeneity.[2] However, genomic analysis of the metastatic process in canine OMMs is still in its infancy. In another recent study, podoplanin, a cell-surface protein that modulates signal transductions that regulate cell proliferation, differentiation, migration, invasion, epithelial-to-mesenchymal transition,[62] was also identified as a driver protein for ameboid invasion in both human and canine mucosal melanoma, hence promoting tumor progression and metastasis.[57]

The aim of the present study was to investigate the molecular basis of canine OMM lymph node metastasis, evaluating differences in gene expression between primary OMMs and matched regional lymph nodal metastases by microarray mRNA profiling and quantitative RT-PCR.

MATERIALS AND METHODS

Case selection and sample collection

Formalin-fixed paraffin-embedded (FFPE) samples of canine primary OMMs and regional lymph node metastases from 13 dogs were retrospectively selected from diagnostic histopathology archives [Pathology Department at the Animal Health Trust (UK) and Department of Pathobiology at the University of Utrecht (the Netherlands)]. Tissue samples were surgically excised from dogs (between 2012 and 2018) for treatment and staging purposes. The confirmed diagnosis of both primary OMMs and metastatic OMMs was obtained by microscopic examination of H&E-stained sections by a board-certified pathologist (SDP). Histological evidence of lymph node metastasis was defined as the presence of large groups of neoplastic cells showing a mass effect on the lymphoid tissue, or the presence of small cohesive groups (>5 cells per high power field/400x) of pleomorphic cells containing melanin pigment. One single representative block was selected from each of the primary OMMs and their lymph node metastasis. Each neoplastic area was outlined using a fine-point permanent marker. A piece of Parafilm large enough to cover the region of interest was placed on the H&E-stained slide. Using a fine-point permanent marker, the entire tissue and the region of interest within the tissue were outlined on the parafilm. The marked parafilm was then transferred to the corresponding FFPE tissue block, matching the outline with the shape of the OMM tissue in the block. Using the tip of a permanent marker, shallow but visible indentations were drawn along the outline of the region of interest. Three tissue cores were extracted from the highlighted area of each FFPE block using a 3.0 mm Miltex Biopsy punch with plunger (Agar Scientific, UK).

RNA isolation, purification and quantification

Total RNA was isolated from all three tissue cores obtained for each FFPE primary OMM and matched lymph node metastasis using the RecoverAll Total Nucleic Acid Isolation Kit (ThermoFisher Scientific, Paisley, UK). OMM RNA samples were further purified (i.e. to

remove melanin) by spin column filtration (OneStep PCR Inhibitor Removal Kit; Zymo Research, Freiburg, Germany). Total RNA concentration was measured by spectrophotometry (NanoDrop 1000 Spectrophotometer, ThermoFisher Scientific), followed by fluorometry assay (Quant-iT RiboGreen RNA Assay Kit, ThermoFisher Scientific).

Global gene expression profiling

RNA amplification, labelling and microarray hybridization

Fragmented, biotinylated single-stranded cDNA was prepared from 29 ng of each of 4 FFPE primary OMMs and matched metastasis RNA samples using the GeneChip WT Pico Reagent Kit (ThermoFisher Scientific).

A mixture of 4 unlabeled synthetic RNAs was added (at the beginning of the procedure) to each tumor RNA sample to act as 'labelling controls', and a mixture of 4 labelled bacterial DNAs was added (at the end of the procedure) to each labelled tumor cDNA sample to act as hybridization controls. Each cDNA was individually hybridized to an array in a Canine Gene 1.1 ST Array Strip (ThermoFisher Scientific), in a proprietary hybridization cocktail (ThermoFisher Scientific). Array strip washing and streptavidin- phycoerythrin staining were undertaken by the GeneAtlas System (ThermoFisher Scientific) Fluidics Station, and array scanning by the GeneAtlas System (ThermoFisher Scientific)

Microarray data analysis

Exon-level probe set expression values were generated by quantile normalization, log2 transformation and signal summarization, performed using the RMA algorithm [29], implemented within 'Affymetrix Expression Console Software 1.3' (ThermoFisher Scientific). 'Outlier arrays' were considered to be those that had any single sample quality, labelling quality and hybridization quality metric value ≥2 standard deviations away from

the mean of the metric value for all the arrays.[73] Outlier arrays were excluded, and processing of the raw probe-level signal intensity data was repeated to generate both quantile normalized and log2-transformed exon and gene-level probe set expression values. Gene-level probe sets ('Transcript clusters') with 'crosshyb_type' = 1 (unique hybridization target) and 'category' = 'main' annotations[74], and for which at least 10% of its exons was 'present' (detection above background p-value <0.01[75]) in at least ≥2 of the primary OMMs and ≥2 of the primary OMM lymph node metastases, were considered to be expressed and used for subsequent analyses.

The similarity between the global expression profiles of primary and lymph node OMMs was visualized by hierarchical clustering performed using WebMeV.[19] Transcript clusters displaying statistically significant differential expression between primary OMM and lymph node metastases were identified by moderated T-test (p-value < 0.05) performed using the R Limma package.[37,72] P-values were adjusted by permutation testing[9] to compensate for "chance" p-values of 0.05 obtained due to multiple testing. Transcription clusters demonstrating a >2-fold difference in median expression level between primary OMM and lymph node metastases were subject to further analysis.

Functional annotation enrichment analysis

The biological processes and pathways overrepresented amongst genes with different expression, comparing primary OMMs and OMM lymph node metastases, were identified using DAVID.[17,27] The functional annotations associated with differentially expressed genes were compared with those ascribed to all Transcript clusters ('crosshyb_type' = 1 and 'category' = 'main') for which the expression of at least 10% of its exons was detected above background in ≥2% of the tumors in the primary OMMs and metastatic OMMs cohort, and over-represented biological processes and pathways identified.

Quantitative RT-PCR analysis

cDNA synthesis

Total RNA (80 ng) was reverse transcribed in 20 µL reactions using the iSCRIPT™ cDNA Synthesis Kit (Bio-Rad, Hercules, CA, USA) according to the manufacturer's instructions.[52] Controls reactions without reverse transcriptase (RT-) were included to enable checking for genomic DNA contamination.

Gene-specific preamplification and quantitative PCR (qPCR)

To increase the sensitivity of qPCR analysis, for each cDNA sample a 20 µL preamplification reaction was performed using 3 µL of cDNA diluted 1:10 (equivalent to 0.4 ng of RNA), 1 µL of TaqMan Gene Expression Assay (Table 1), 10 µL of SsoAdvanced™ Preamp Supermix (Bio-Rad, Hercules, CA, USA). Preamplification reactions were run for 3 min at 95°C, followed by 10 cycles of 15 s at 95°C and 4 min at 58 ◦C.

QPCR amplification was performed using 1 µL of preamplification reaction product, 10 µL of SsoAdvanced Universal Probes Supermix (Bio-Rad, Hercules, CA), 1 µL of TaqMan Gene Expression Assay (Table 1), and RNase-free water to a final volume of 20 µl. QPCR cycling conditions included an initial denaturation step of 15 s at 95°C, followed by 40 cycles at 95°C for 5 s and at 60°C for 30 s. RT- controls were enrolled in the qPCR to check for potential genomic DNA contamination. Both preamplification and amplification reactions were run in 96-well optical plates on a StepOne Plus Real-time PCR instrument (Applied Biosystems, California, USA). Three technical replicate qPCR reactions were performed for each preamplified cDNA sample, and the mean Cq value calculated from values determined using StepOne Software v2.3 (Applied Biosystems, California, USA). QPCR amplification efficiency was assessed as previously described.[40] The 'Livak method' was used to calculate normalized value (2^-ΔCq) of the target genes[38].

Selection of endogenous control reference genes for relative quantification of gene expression

Following the MIQE guidelines[8], qPCR analysis requires data normalization with the most stably expressed endogenous control (EC) genes to minimize data variation that can mask or exaggerate biological changes. Three candidate genes were chosen as a potential EC: ACTB, GAPDH and RPS18. Candidate ECs expression stabilities were examined with four algorithms, comparative ΔCq method[58], BestKeeper[50], NormFinder[1], and GeNorm[67]. The RefFinder tool[71] was used to compare and integrate the output data of the four algorithms, and rank the candidate ECs in the order of the decreasing stability of their expression across all the RNA samples[21].

Statistical analysis

Statistical analysis was performed on normally distributed 2^-ΔCq values. Gene expression data were analyzed using an unpaired t-test to compare the normalized expression value (2^-ΔCq) of selected genes in metastatic OMM *versus* primary OMM cases. Statistical analyses were performed with GraphPad Prism 9 (GraphPad, San Diego, CA, USA). Statistical significance occurred when $P < 0.05$.

Results

Total RNA yields and purity

Total RNAs isolated from OMM FFPE biopsies were of high purity, with OD260/280nm ratios ranging from 1.9 - 2.0, and OD260/230nm ratios from 1.9 to 2.2. Total RNA yields varied between 50 and 100 ng.

Tumors included in differential gene expression analysis

In order to define changes in the gene expression profiles of primary OMMs associated with the process of metastatic dissemination to a regional lymph node, comparative global gene expression analysis of biopsies of canine primary OMMs (4) and their lymph node metastases (4) was performed. The use of matched primary and metastatic tumors intended to minimise potential confounding effects of tumor genetic heterogeneity.

The microarray expression data for one lymph node metastasis sample ('3S') was excluded from the analysis because it was an "outlier array" (see Materials and Methods), having an 'all_probeset_rle_mean' quality metric value 2.24 standard deviations away from the mean of the metric value of all the arrays.

The gene-level probe set expression values obtained for 4 primary and 3 metastatic OMMs were compared for 9,964 Transcript clusters (category = main; crosshyb_type = 1). A Transcript cluster was considered to be present if ≥10% of its exons were present both in ≥2 primary OMMs and ≥2 metastatic OMMs. Unsupervised hierarchical clustering of the 4 primary OMMs and 3 OMM lymph node metastases on the basis of the expression levels of the 9,964 genes suggested a higher degree of similarity between unrelated OMM lymph node metastases, and between different primary OMMs, respectively, than between a primary OMM and its derivative lymph node metastasis (Figure 1).

Genes displaying differential expression between primary and metastatic OMMs

In total, 501 Transcript Clusters (genes) displayed a statistical difference in expression (p-value <0.05) between primary and metastatic OMMs, after permutation testing-adjustment. A >2-fold change (median primary/median metastatic expression value or median metastatic/median primary expression value) was considered to be authentic and more likely to be reproducibly measurable. Greater than 2-fold differences in expression between the primary and OMM metastases were exhibited by 151 genes, with 13

displaying increased expression and 16 decreased expression, respectively, in the lymph node metastases (Figure 2 and Supplementary Table 1).

Functional annotation enrichment analysis:

The frequencies of functional annotations assigned to 148 of the 158 Transcription Clusters that were differentially expressed between the primary and metastatic OMMs, and which had unique Ensembl canine gene IDs, were compared with those associated with all the Transcript Clusters expressed by the OMMs (9,123 of 9,964 which had associated Ensembl canine gene IDs). Over-represented amongst the genes exhibiting differential expression were 4 Gene Ontology Consortium biological processes and 4 KEGG pathways potentially involved in the metastatic process (Table 2).

RT-qPCR assessment of differential gene expression

The relative expression levels of selected genes were derived using the normalized value 2^- (Cq target gene – Cq reference gene) values. ACTB was selected as the best endogenous control, with respect to GAPDH and RPS18, by utilizing four mathematical approaches: comparative ΔCq method, BestKeeper, NormFinder, and GeNorm (Table 3).[21] RT-qPCR analysis featured 13 pairs of primary OMMs and their lymph node metastases, including the 4 sample pairs subject to global gene expression profiling, and 10 subsequently collected primary tumor: lymph node metastasis sample pairs. The analysis sought to confirm the differential expression of 7 selected genes directly associated with Rac1 activation (Figure 3). The statistically significant >2-fold increased median expression of CORO1A, ITGA4 and VAV3 in the lymph node metastases determined by microarray-based transcriptional profiling was validated by RT-qPCR. RT-qPCR assay also confirmed the 'direction' of the >2-fold difference in the median expression of ELMO1 (increased expression in OMM lymph node metastases), and SPARC and MMP2 (both decreased

expression in OMM lymph node metastases), in accordance with the results of the microarray analysis, although the differences in expression did not reach statistical significance. DOCK2 exhibited statistically significant >2-fold decreased median expression in the lymph node metastases, in contrast to the >2-fold increased median expression observed in the lymph node metastases in the 4 sample-pair microarray investigation.

DISCUSSION

OMM is the most common malignant cancer of the oral cavity in the dog,[22,46] with frequent metastases and poor prognosis. The propensity of OMMs to metastasise is likely to be associated with pro-metastatic changes in gene expression in primary tumor cells.[5] Identification of these alterations holds the key to pinpointing potential targets for the control and treatment of OMM metastatic dissemination. Thus, this study aimed to identify potentially metastasis-associated differences in gene expression between canine primary OMMs and their relative regional lymph nodal metastases.

Several of the genes exhibiting differential expression between primary and metastatic OMMs are associated with cell motility, and are directly and/or indirectly involved in the regulation of the Rac1 signaling-associated genes.[32,35,39,41] Variation in the expression of these genes are also frequently correlated with highly aggressive tumor subtypes in humans.[11,14,35,39]

Rac1 (Ras-related C3 botulinum toxin substrate 1) is the major ubiquitous isoform of Rac expressed in mammalian tissue, as part of the Rho family of small GTPases, which controls assembly of the cellular actin cytoskeleton. Lamellipodia are actin polymerisations at the leading edge of cells, representing the main force for cell migration, and their formation is under the control of Rac1. Indeed, loss of Rac1 in tissues and cell cultures leads to the loss of lamellipodia and a general reduction of migration speed.[33] The results

of our study support the hypothesis that activation of downstream effectors and upstream regulators of Rac1 may facilitate canine OMM cell migration to a regional lymph node. This study highlighted the increased expression in canine OMM lymph node metastases of a number of genes involved with cell migration-associated Rac1 signaling.

VAV3 is a member of the VAV gene family. VAV proteins activate pathways leading to actin cytoskeletal rearrangements, mainly acting as a guanine nucleotide exchange factor for RhoG, RhoA and Rac1. Elevated VAV3 expression has been linked to prostate cancer progression and post-treatment recurrence,[36] to glioblastoma cell migration, invasion and proliferation and also to a shorter overall survival[42], lymphatic metastasis and perineural invasion in gastric cancer.[64] Microarray and RT-qPCR-determined increased expression in lymph node metastases indicate that this gene may also be involved in canine OMM progression.

Coronin1A (encoded by the *CORO1A* gene) plays a pivotal role in the cytoskeleton in highly motile cells, contributing to the formation of plasma membrane protrusions essential for cell locomotion. Notably, this protein is particularly enriched in haematopoietic tissues.[47] Overexpression of CORO1A prompts the translocation of Rac1 to the plasma membrane, favouring its activation.[12] We hypothesize that the increased expression of CORO1A may be associated with the acquisition of a highly motile phenotype in OMM cells, as previously suggested in human mammary tumors.[31]

Integrin alpha 4 (ITGA4) mediates cell-cell adhesion important in immune function. ITGA4 is also widely expressed in neural crest cells, leukocytes, striated and smooth muscle, and neurons, and mediates their migration, most likely co-localising and activating Rac1[48]. A recent study on human cutaneous melanoma suggests that ITGA4 is closely related to the occurrence and development of melanoma, and that it can promote the metastasis of melanoma by favoring the aggregation of melanoma cells in the lymphatic system.[49]

309 Moreover, overexpression of ITGA4 has been demonstrated in human gastrointestinal
310 stromal tumors, where it is associated with an unfavourable prognosis[53].
311 Dock2 (Dedicator Of Cytokinesis 2) is a member of the CDM family of proteins, known to
312 regulate the actin cytoskeleton by functioning upstream of Rac1.[65] DOCK2 activates Rac1
313 and regulates the actin cytoskeleton through a self-inhibiting interaction with ELMO1.[13,55]
314 Proteins encoded by *ELMO1* interact with dedicator of cytokinesis proteins to promote
315 phagocytosis and cell migration[30]. Mutation-effected aberrant activation of *ELMO1* and
316 *DOCK2* has been reported in human oesophageal adenocarcinoma, a highly invasive
317 tumor prone to early metastasis.[18] RT-qPCR assay did not confirm the >2-fold increase in
318 median DOCK2 expression in OMM lymph node metastases determined by microarray
319 gene expression profiling.
320 Although several RAC1 signaling-associated genes displayed increased expression in
321 OMM lymph node metastases, RT-qPCR assay suggested that this was not the case for
322 MMP2, and SPARC, respectively. Downregulation of SPARC expression is related to the
323 Rac1 signaling-associated pathways. Secreted protein acidic and cysteine-rich (SPARC,
324 also known as osteonectin) is a matrix-associated protein, usually playing a role in bone
325 mineralisation, regulating cell interaction with the extracellular milieu during development
326 and in response to injury.[7] SPARC expression has been associated with an aggressive,
327 mesenchymal-like phenotype in a variety of human cancers, including melanoma. In
328 particular, its expression in melanoma cells was associated with decreased E-cadherin
329 and increased N-cadherin expression levels suggesting that this protein may regulate
330 epithelial–mesenchymal transition[51]. However, there is evidence that SPARC is a
331 permissive factor for Rac1 that becomes fully active only when SPARC levels are low;
332 indeed, suppression of SPARC expression induces the formation of lamellipodia
333 extension.[54] The potentially decreased SPARC expression in canine OMM lymph node
334 metastases demonstrated herein is conceptually consistent with the latter finding, although

335 further investigation of a possible role for SPARC in canine OMM metastasis is warranted.
336 Matrix metallopeptidase 2 (MMP-2) is an enzyme able to cleave components of the
337 extracellular matrix, precisely gelatin type I and collagen types IV, V, VII and X. It has been
338 shown that Membrane Type 1 Metalloprotease (MT1-MMP), highly expressed in neural
339 crest cells, mediates human melanoma cell invasion through the activation of its target
340 MMP-2 and, in turn, MMP-2 activation is required to sustain Rac1 activity and promote cell
341 migration.[56]
342 Rac1 is also implicated in epithelial-mesenchymal transition (EMT), inducing
343 downregulation of E-cadherin and upregulation of N-cadherin, vimentin, and SNAIL1 in
344 human cancers.[70] Melanocytes do not belong to the epithelial lineage and therefore the
345 term EMT cannot be formally attributed to the progression of malignant melanoma.
346 However, various studies have demonstrated that melanoma cells display EMT-like
347 phenotype switching, both in humans and dogs.[34,59,68] Indeed, differentiated melanocytes
348 do express E-cadherin and loss of this protein, which represents a hallmark of EMT in
349 epithelial tumors, is also evident in late-stage malignant melanomas, especially in nodal
350 metastases[44].
351 RAC1 has been identified as an oncogene in human cutaneous melanoma.[61] In particular,
352 the p.P29S hot spot mutation likely destabilises RAC1 favouring its active GTP-bound
353 state.[26] Intriguingly, both $RAC1^{P29S}$ mutant melanoma cells and RAC1 wild type melanoma
354 cells reduce their proliferation by downregulation of Rac1.[28] However, RAC1 mutations
355 have not been found in human mucosal melanomas, or in primary and metastatic canine
356 OMMs.[69] Beyond the p.P29S missense mutation, Rac1 is activated by other molecular
357 mechanisms in human cutaneous melanoma.[16] Some of these mechanisms may be
358 similar to the putative Rac1 activation-promoting gene expression changes identified in the
359 current study. This study has demonstrated that canine OMM lymph node metastases are
360 characterized by increased expression (relative to primary OMMs) of a set of genes

involved in cell motility, in particular genes involved in Rac1 signaling. The potential key role of Rac1 and its upstream activators and downstream effectors in the modulation of critical elements of metastasis has been highlighted, as it has been done previously in human medicine.[3] It is possible that melanoma cells are able to disseminate to distant sites due to re-acquisition of plastic and highly migratory behaviour characteristic of their embryonic precursors.[23] Rac1 activation could be one of these mechanisms as it is essential for lamellipodia formation. Indeed, lamellipodia formation is also used by dendritic cells to interact with the endothelium, polarise, and actively crawl toward the draining lymph node.[63]

The main limitation of this study is the relatively low number of primary OMMs and lymph node metastasis biopsy pairs analysed. Fine needle aspiration (FNA) remains a mainstay diagnostic technique when evaluating for metastasis to regional lymph nodes in animals, being less invasive compared to surgical excision and frequently preferred to histological examination of the lymph node, despite the latter technique being considered the gold standard for the identification of nodal metastasis[20]. Moreover, dogs with OMM are often inoperable at diagnosis, hence, cytology would be the only viable option to provide a complete staging. Therefore, there are only a limited number of instances where both a primary OMM and a regional lymph node biopsy are available. A further constraint is that it was necessary to use FFPE tissue biopsies. Degradation of RNA by formalin fixation is well known, and probably mainly affects the accurate quantification of genes expressed at low levels.

The role of Rac1 signaling in tumorigenesis, angiogenesis, invasion, and metastasis has been demonstrated for several different human tumor types[3], and it may have a similarly important role in canine OMM development and progression. Targeting Rac1 and its regulatory network would be beneficial for cancer treatment, but this has unfortunately proved to be difficult. Rac1 signaling is involved in many processes of normal cell

physiology, including cellular plasticity, migration and invasion, cellular adhesions, cell proliferation, apoptosis, reactive oxygen species (ROS) production and immune responses.[4] Therefore, targeting Rac1 in a clinical setting might bear undesirable side effects. Investigation of both the downstream effectors and the upstream regulators of Rac1 could indicate the best unimodal/multimodal therapeutic approaches for canine OMMs. At this stage, additional validation in different preclinical cancer models is needed to supplement the striking *in vitro* evidence of the potential benefits of targeting Rac1.[41]

Ethics statement

This study (Project number 59-2016) was approved by the Animal Health Trust (AHT) Ethics Committee. Informed, written consent was obtained from the owners of dogs whose oral melanoma and lymph nodal biopsies were included in this study. A melanoma/lymph node biopsy could be withdrawn from the study at any time. Patient treatment was unaffected by the study.

REFERENCES

1. Andersen CL, Jensen JL, Ørntoft TF. Normalization of real-time quantitative reverse transcription-PCR data: a model-based variance estimation approach to identify genes suited for normalization, applied to bladder and colon cancer data sets. *Cancer Res*. 2004;**64**(15):5245–5250.
2. Argyris PP, Naumann J, Jarvis MC, et al. Primary mucosal melanomas of the head and neck are characterised by overexpression of the DNA mutating enzyme APOBEC3B. *Histopathology*. 2023;**82**(4):608–621.
3. Bid HK, Roberts RD, Manchanda PK, Houghton PJ. RAC1: An emerging therapeutic option for targeting cancer angiogenesis and metastasis. *Molecular Cancer Therapeutics*. 2013:
4. Bosco EE, Mulloy JC, Zheng Y. Rac1 GTPase: A "Rac" of all trades. *Cellular and Molecular Life Sciences*. 2009:
5. Bowlt Blacklock KL, Birand Z, Selmic LE, et al. Genome-wide analysis of canine oral malignant melanoma metastasis-associated gene expression. *Sci Rep*. 2019;**9**(1):6511.
6. Brachelente C, Cappelli K, Capomaccio S, et al. Transcriptome Analysis of Canine Cutaneous Melanoma and Melanocytoma Reveals a Modulation of Genes Regulating Extracellular Matrix Metabolism and Cell Cycle. *Sci Rep*. 2017;**7**(1):6386.
7. Bradshaw AD, Sage EH. SPARC, a matricellular protein that functions in cellular differentiation and tissue response to injury. *J Clin Invest*. 2001;**107**(9):1049–1054.
8. Bustin SA, Benes V, Garson JA, et al. The MIQE Guidelines: Minimum Information for Publication of Quantitative Real-Time PCR Experiments. *Clin Chem*. 2009;**55**(4):611–622.

9. Camargo A, Azuaje F, Wang H, Zheng H. Permutation – based statistical tests for multiple hypotheses. *Source Code Biol Med*. 2008;**3**(1):15.
10. Cambier S, Gouwy M, Proost P. The chemokines CXCL8 and CXCL12: molecular and functional properties, role in disease and efforts towards pharmacological intervention. *Cell Mol Immunol*. 2023;**20**(3):217–251.
11. Cannon AC, Uribe-Alvarez C, Chernoff J. RAC1 as a Therapeutic Target in Malignant Melanoma. *Trends Cancer*. 2020;**6**(6):478–488.
12. Castro-Castro A, Ojeda V, Barreira M, et al. Coronin 1A promotes a cytoskeletal-based feedback loop that facilitates Rac1 translocation and activation. *EMBO J*. 2011.
13. Chang L, Yang J, Jo CH, et al. Structure of the DOCK2−ELMO1 complex provides insights into regulation of the auto-inhibited state. *Nat Commun*. 2020;**11**(1):3464.
14. Chen M, Li H, Xu X, et al. Identification of RAC1 in promoting brain metastasis of lung adenocarcinoma using single-cell transcriptome sequencing. *Cell Death Dis*. 2023;**14**(5):1–14.
15. Chiang AC, Massagué J. Molecular Basis of Metastasis. *N Engl J Med*. 2008;**359**(26):2814–2823.
16. Colón-Bolea P, García-Gómez R, Casar B. RAC1 Activation as a Potential Therapeutic Option in Metastatic Cutaneous Melanoma. *Biomolecules*. 2021;**11**(11):1554.
17. Dennis G, Sherman BT, Hosack DA, et al. DAVID: Database for Annotation, Visualization, and Integrated Discovery. *Genome Biol*. 2003;**4**(5):P3.
18. Dulak AM, Stojanov P, Peng S, et al. Exome and whole-genome sequencing of esophageal adenocarcinoma identifies recurrent driver events and mutational complexity. *Nat Genet*. 2013.
19. Eisen MB, Spellman PT, Brown PO, Botstein D. Cluster analysis and display of genome-wide expression patterns. *Proc Natl Acad Sci U S A*. 1998;**95**(25):14863–14868.
20. Grimes JA, Matz BM, Christopherson PW, et al. Agreement Between Cytology and Histopathology for Regional Lymph Node Metastasis in Dogs With Melanocytic Neoplasms. *Vet Pathol*. 2017.
21. Guelfi G, Capaccia C, Santoro MM, Diverio S. Identification of Appropriate Endogenous Controls for Circulating miRNA Quantification in Working Dogs under Physiological Stress Conditions. *Animals*. 2023;**13**(4):576.
22. Guth AM, Dow S. *Withrow and MacEwen's Small Animal Clinical Oncology*. *Withrow and MacEwen's Small Animal Clinical Oncology, 5/e*. Elsevier 2013.
23. Hendrix MJC, Seftor EA, Seftor REB, Kasemeier-Kulesa J, Kulesa PM, Postovit LM. Reprogramming metastatic tumour cells with embryonic microenvironments. *Nat Rev Cancer*. 2007;**7**(4):246–255.
24. Hendrix MJC, Seftor EA, Seftor REB, Kasemeier-Kulesa J, Kulesa PM, Postovit L-M. Reprogramming metastatic tumour cells with embryonic microenvironments. *Nat Rev Cancer*. 2007;**7**(4):246–255.
25. Heppt MV, Wang JX, Hristova DM, et al. MSX1-Induced Neural Crest-Like Reprogramming Promotes Melanoma Progression. *J Invest Dermatol*. 2018;**138**(1):141–149.
26. Hodis E, Watson IR, Kryukov G V., et al. A landscape of driver mutations in melanoma. *Cell*. 2012;**150**(2):251–263.
27. Huang DW, Sherman BT, Lempicki RA. Systematic and integrative analysis of large gene lists using DAVID bioinformatics resources. *Nat Protoc*. 2009;**4**(1):44–57.
28. Immisch L, Papafotiou G, Gallarín Delgado N, et al. Targeting the recurrent Rac1P29S neoepitope in melanoma with heterologous high-affinity T cell receptors. *Front Immunol*. 2023;**14**:1119498.
29. Irizarry RA, Bolstad BM, Collin F, Cope LM, Hobbs B, Speed TP. Summaries of Affymetrix GeneChip probe level data. *Nucleic Acids Res*. 2003;**31**(4):e15.
30. Jiang J, Liu G, Miao X, Hua S, Zhong D. Overexpression of engulfment and cell motility 1 promotes cell invasion and migration of hepatocellular carcinoma. *Exp Ther Med*. 2011;**2**(3):505–511.

31. Kim D-H, Bae J, Lee JW, et al. Proteomic analysis of breast cancer tissue reveals upregulation of actin-remodeling proteins and its relevance to cancer invasiveness. *Proteomics Clin Appl*. 2009;**3**(1):30–40.
32. ten Klooster JP, Leeuwen I v, Scheres N, Anthony EC, Hordijk PL. Rac1-induced cell migration requires membrane recruitment of the nuclear oncogene SET. *EMBO J*. 2007;**26**(2):336–345.
33. Li A, Ma Y, Yu X, et al. Rac1 Drives Melanoblast Organization during Mouse Development by Orchestrating Pseudopod- Driven Motility and Cell-Cycle Progression. *Dev Cell*. 2011.
34. Li FZ, Dhillon AS, Anderson RL, McArthur G, Ferrao PT. Phenotype Switching in Melanoma: Implications for Progression and Therapy. *Front Oncol*. 2015;**5**.
35. Liang J, Oyang L, Rao S, et al. Rac1, A Potential Target for Tumor Therapy. *Front Oncol*. 2021;**11**.
36. Lin KT, Gong J, Li CF, et al. Vav3-Rac1 signaling regulates prostate cancer metastasis with elevated Vav3 expression correlating with prostate cancer progression and posttreatment recurrence. *Cancer Res*. 2012.
37. Liu W, Peng Y, Tobin DJ. A new 12-gene diagnostic biomarker signature of melanoma revealed by integrated microarray analysis. *PeerJ*. 2013;**2013**(1):1–23.
38. Livak KJ, Schmittgen TD. Analysis of Relative Gene Expression Data Using Real-Time Quantitative PCR and the 2−ΔΔCT Method. *Methods*. 2001;**25**(4):402–408.
39. Ma N, Xu E, Luo Q, Song G. Rac1: A Regulator of Cell Migration and a Potential Target for Cancer Therapy. *Molecules*. 2023;**28**(7):2976.
40. Mandara M t., Reginato A, Foiani G, De Luca S, Guelfi G. Gene Expression of Matrix Metalloproteinases and their Inhibitors (TIMPs) in Meningiomas of Dogs. *J Vet Intern Med*. 2017;**31**(6):1816–1821.
41. Marei H, Malliri A. Rac1 in human diseases: The therapeutic potential of targeting Rac1 signaling regulatory mechanisms. *Small GTPases*. 2017;**8**(3):139–163.
42. Miao R, Huang D, Zhao K, et al. VAV3 regulates glioblastoma cell proliferation, migration, invasion and cancer stem-like cell self-renewal. *Mol Med Rep*. 2023;**27**(4):94.
43. Mikiewicz M, Paździor-Czapula K, Gesek M, Lemishevskyi V, Otrocka-Domagała I. Canine and Feline Oral Cavity Tumours and Tumour-like Lesions: a Retrospective Study of 486 Cases (2015-2017). *J Comp Pathol*. 2019;**172**:80–87.
44. Miller AJ, Mihm MC. mechanisms of disease Melanoma. *N Engl J O F Med*. 2006.
45. Munday JS, Löhr CV, Kiupel M. Tumors of the Alimentary Tract. *Wiley Online Library*. John Wiley & Sons, Ltd 2016:499–601.
46. Munday JS, Löhr C V., Kiupel M. Tumors of the Alimentary Tract. In: *Tumors in Domestic Animals*. John Wiley & Sons, Inc. 2016:500.
47. Nal B, Carroll P, Mohr E, et al. Coronin-1 expression in T lymphocytes: insights into protein function during T cell development and activation. *Int Immunol*. 2004;**16**(2):231–240.
48. Nishiya N, Kiosses WB, Han J, Ginsberg MH. An α4 integrin-paxillin-Arf-GAP complex restricts Rac activation to the leading edge of migrating cells. *Nat Cell Biol*. 2005;**7**(4):343–352.
49. Nurzat Y, Su W, Min P, Li K, Xu H, Zhang Y. Identification of Therapeutic Targets and Prognostic Biomarkers Among Integrin Subunits in the Skin Cutaneous Melanoma Microenvironment. *Front Oncol*. 2021;**11**:751875.
50. Pfaffl MW, Tichopad A, Prgomet C, Neuvians TP. Determination of stable housekeeping genes, differentially regulated target genes and sample integrity: BestKeeper – Excel-based tool using pair-wise correlations. *Biotechnol Lett*. 2004;**26**(6):509–515.
51. Podhajcer OL, Benedetti LG, Girotti MR, Prada F, Salvatierra E, Llera AS. The role of the matricellular protein SPARC in the dynamic interaction between the tumor and the host. *Cancer Metastasis Rev*. 2008;**27**(4):691–705.
52. Porcellato I, Brachelente C, Guelfi G, et al. A Retrospective Investigation on Canine Papillomavirus 1 (CPV1) in Oral Oncogenesis Reveals Dogs Are Not a Suitable Animal Model for

High-Risk HPV-Induced Oral Cancer. *PLOS ONE*. 2014;**9**(11):e112833.
53. Pulkka OP, Mpindi JP, Tynninen O, et al. Clinical relevance of integrin alpha 4 in gastrointestinal stromal tumours. *J Cell Mol Med*. 2018;**22**(4):2220–2230.
54. Salvatierra E, Alvarez MJ, Leishman CC, et al. SPARC controls melanoma cell plasticity through Rac1. *PLoS ONE*. 2015.
55. Sanui T, Inayoshi A, Noda M, et al. DOCK2 regulates Rac activation and cytoskeletal reorganization through interaction with ELMO1. *Blood*. 2003.
56. Shaverdashvili K, Wong P, Ma J, Zhang K, Osman I, Bedogni B. MT1-MMP modulates melanoma cell dissemination and metastasis through activation of MMP2 and RAC1. *Pigment Cell Melanoma Res*. 2014;**27**(2):287–296.
57. Shinada M, Kato D, Motegi T, et al. Podoplanin Drives Amoeboid Invasion in Canine and Human Mucosal Melanoma. *Mol Cancer Res*. 2023;**21**(11):1205–1219.
58. Silver N, Best S, Jiang J, Thein SL. Selection of housekeeping genes for gene expression studies in human reticulocytes using real-time PCR. *BMC Mol Biol*. 2006;**7**(1):33.
59. Silvestri S, Porcellato I, Mechelli L, et al. E-Cadherin Expression in Canine Melanocytic Tumors: Histological, Immunohistochemical, and Survival Analysis. *Vet Pathol*. 2020;**57**(5):608–619.
60. Smith SH, Goldschmidt MH, McManus PM. A comparative review of melanocytic neoplasms. *Vet Pathol*. 2002;**39**(6):651–678.
61. Sondka Z, Dhir NB, Carvalho-Silva D, et al. COSMIC: a curated database of somatic variants and clinical data for cancer. *Nucleic Acids Res*. 2024;**52**(D1):D1210–D1217.
62. Suzuki H, Kaneko MK, Kato Y. Roles of Podoplanin in Malignant Progression of Tumor. *Cells*. 2022;**11**(3):575.
63. Tal O, Lim HY, Gurevich I, et al. DC mobilization from the skin requires docking to immobilized CCL21 on lymphatic endothelium and intralymphatic crawling. *J Exp Med*. 2011;**208**(10):2141–2153.
64. Tan B, Li Y, Shi X, et al. Expression of Vav3 protein and its prognostic value in patients with gastric cancer. *Pathol - Res Pract*. 2017;**213**(5):435–440.
65. Terasawa M, Uruno T, Mori S, et al. Dimerization of DOCK2 Is Essential for DOCK2-Mediated Rac Activation and Lymphocyte Migration. *PLoS ONE*. 2012;**7**(9):1–7.
66. Valastyan S, Weinberg RA. Tumor metastasis: molecular insights and evolving paradigms. *Cell*. 2011;**147**(2):275–292.
67. Vandesompele J, De Preter K, Pattyn F, et al. Accurate normalization of real-time quantitative RT-PCR data by geometric averaging of multiple internal control genes. *Genome Biol*. 2002;**3**(7):RESEARCH0034.
68. Veloso ES, Gonçalves INN, Silveira TL, et al. ZEB and Snail expression indicates epithelial-mesenchymal transition in canine melanoma. *Res Vet Sci*. 2020;**131**:7–14.
69. Wong K, van der Weyden L, Schott CR, et al. Cross-species genomic landscape comparison of human mucosal melanoma with canine oral and equine melanoma. *Nat Commun*. 2019;**10**(1):353.
70. Xia L, Lin J, Su J, et al. Diallyl disulfide inhibits colon cancer metastasis by suppressing Rac1-mediated epithelial-mesenchymal transition . *OncoTargets Ther*. 2019.
71. Xie F, Xiao P, Chen D, Xu L, Zhang B. miRDeepFinder: a miRNA analysis tool for deep sequencing of plant small RNAs. *Plant Mol Biol*. 2012.
72. Yang W, Speed T. Design and Analysis of Comparative Microarray Experiments. *Stat Anal Gene Expr Microarray Data*. 2003.
73. QC Metrics for Exon and Gene Design Expression Arrays. A summary based on the Affymetrix Quality Assessment of Exon and Gene Arrays White Paper, http://static1.1. sqspcdn.com/static/f/1438485/21486054/1359060361517/qc_metrics_exon_gene_qrc. pdf.
74. Affymetrix Exon and Gene Array Glossary, https://www.affymetrix.com/support/help/exon_glossary/index.affx.

75. Affymetrix Exon Array Background Correction Revision Date: 2005-09-27, Revision Version: 1.0, https://assets.thermofisher.com/ TFS-Assets/LSG/brochures/exon_background_correction_whitepaper.pdf.

FIGURE 1: Comparison of the global gene expression profiles of primary OMMs and matched lymph node metastases. Hierarchical clustering (average group linkage, distance = 1 - Pearson Correlation Coefficient) of 4 primary OMMs (P) and 3 matched lymph node metastases (M) on the basis of the expression levels of 9,964 genes.

FIGURE 2: Fold differences in the median expression levels (measured by exon microarray) of 501 genes between 4 primary OMMs (P) and 3 matched lymph node metastases (M) are depicted. Red spheres denote 7 genes involved in RAC1 signaling-associated regulation of cell migration, whose differential expression was subsequently assayed by RT-qPCR. The red arrow indicates two genes (CORO1A and DOCK2) that displayed highly similar fold change differences in expression. The dotted line represents a permutation testing-adjusted (PTadj.) t-test p-value of 0.05.

FIGURE 3: PCR normalized expression levels. The figure shows the normalized expression value (2^-ΔCq) of target genes examined in the primary tumor samples (white column) and metastasis samples (gray column). The expression levels of ITGA4, VAV3, and CORO1A genes are significantly higher in metastasis compared to primary tumors. Conversely, DOCK2 shows reduced expression in metastasis compared to primary tumor. ELMO1, SPARC, and MMP2 display no statistically significant difference between the two groups ($p > 0.05$). An unpaired t-test is employed for comparing the two groups of data (metastasis vs primary tumor); *$p < 0.05$; **$p < 0.01$; **$p < 0.001$.

Gene Symbol	Reference Sequence	TaqMan assay ID	Exon boundary	Amplicon (bp)
ITGA4	XM_003502135.1	Cg04426096_m1	20-21	64
SPARC	XM_005619272.4	Cf02661382_m1	5-6	67
CORO1A	XM_547069.7	Cf02706862_m1	9-10	159
VAV3	XM_022420692.1	Cf02705614_m1	11-12	148
DOCK2	XM_546246.5	Cf02703791_m1	15-16	85
ELMO1	XM_005628727.3	Cf00919416_m1	5-6	89
MMP2	XM_014109407.1	Cf01548727_m1	1-2	65
ACTB	NM_001195845.2	Cf04931159_m1	-	52
RPS18	NM_001048082.1	Cf02624916_g1	5-6	99
GAPDH	NM_001003142.2	Cf04419463_gH	5-6	54

Table 1. TaqMan Gene Expression Assays. The table summarizes the TaqMan assays used in the study to detect target genes (white boxes) and candidate normalization control genes (grey boxes). Gene symbol (first column), interrogated transcript sequence (second column), TaqMan probe ID (third column), base co-ordinates of exon-exon junction spanned by the used PCR assay (fourth column), and amplicon length (last column) are listed. All selected probes hybridise to two different exons (except for ACTB) and are specific for *Canis familiaris* mRNA transcripts. Design of the TaqMan assay for ITGA4 was based on the *Cricetulus griseus* CHO-K1 cell line ITGA4 mRNA transcript, however, an antibody raised against the *Cricetulus griseus* ITGA4 protein demonstrates 100% cross-reactivity with the *Canis familiaris ITGA4 protein.*.

Functional annotation	Fold enrichment	P-value	Gene expression	
			M>P	P>M
GO:0045785~positive regulation of cell adhesion	15.187	0.015	*APBB1IP, VAV3*	*CYTH3*
GO:0030036~actin cytoskeleton organization	7.087	0.017	*ELMO1, CORO1A, DOCK2, FMNL1*	
GO:0001768~establishment of T cell polarity	47.249	0.041	*CCL19, DOCK2*	
GO:0007165~signal transduction	4.588	≤0.001	*TRAF5, ERBIN, SPOCK2, CDC42SE2, APBB1IP, LNPEP, FYB*	*SPARC*
cfa04514: Cell adhesion molecules	7.002	≤0.0001	*PTPRC, CD226, ICOS, PECAM1, DLA-DOB, ITGA4, CD2*	
cfa05200: Pathways in cancer	2.741	0.008	*TRAF5, IGF1, PLCB2, CDKN1B, STK4, PLCG2, JAK1, LEF1*	*ADCY2, MMP2*
cfa04062: Chemokine signaling pathway	4.951	≤0.001	*CCR7, PLCB2, ELMO1, CCL19, CXCL13, DOCK2, VAV3*	*ADCY2*

cfa04670: Leukocyte transendothelial migration	5.001	0.015	*PLCG2, PECAM1, VAV3, ITGA4*	*MMP2*

615

616 **Table 2**. Differentially expressed gene-associated enriched functional annotations. GO:

617 Gene Ontology. M: Metastatic OMMs; P: Primary OMMs.

ALGORITHM	**EC RANK**		
Delta Cq	ACTB	GAPDH	RPS18
BestKeeper	GAPDH	ACTB	RPS18
NormFinder	ACTB	GAPDH	RPS18
GeNorm	GAPDH | ACTB		RPS18
RefFinder comprehensive ranking	ACTB	GAPDH	RPS18

618 **Table 3.** RefFinder ranking stability order. The table shows stability values ranking assigned
619 by RefFinder which integrate the data obtained from the comparative ΔCq method,
620 BestKeeper, NormFinder, and GeNorm algorithms. RefFinder tool generates a
621 comprehensive ranking by ordering the candidate endogenous controls from most stable
622 (first column) to least stable (third column).

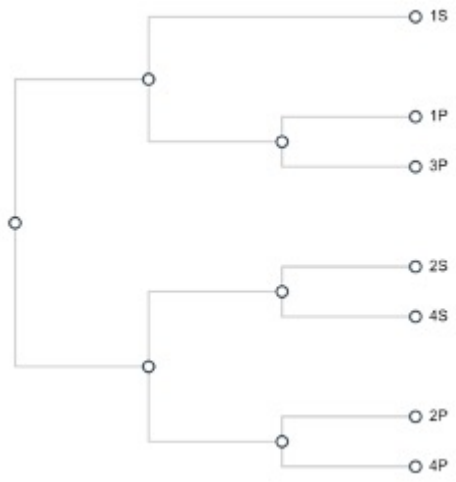

623 Figure 1

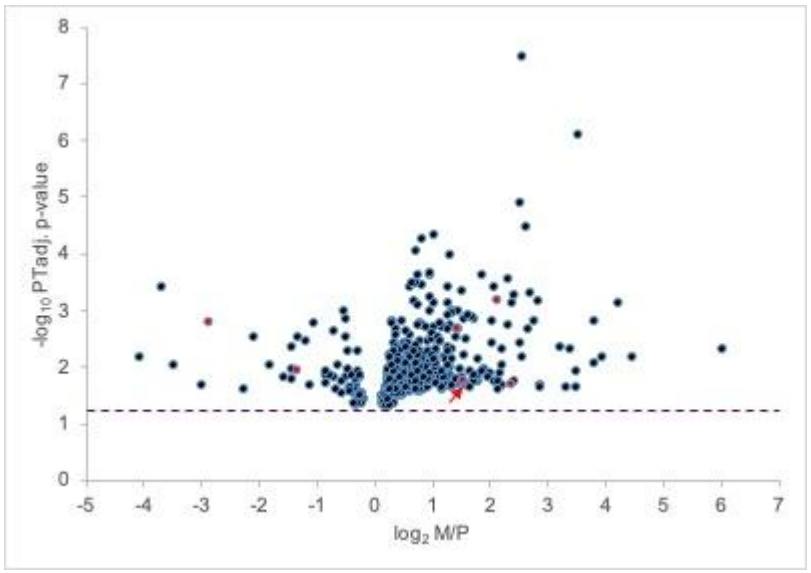

Figure 2

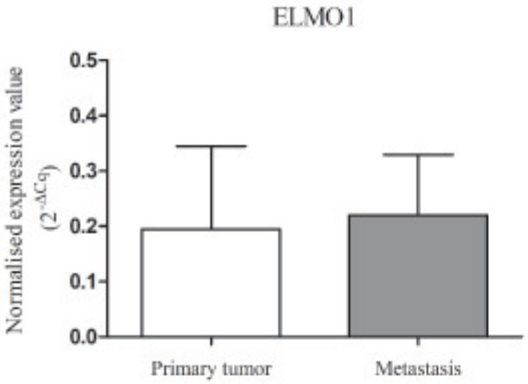
ELMO1
Normalised expression value
(2^-ΔCq)
0.5
0.4
0.3
0.2
0.1
0.0
Primary tumor
Metastasis

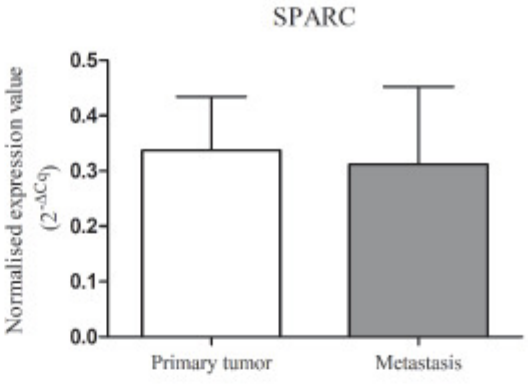
SPARC
Normalised expression value
(2^-ΔCq)
0.5
0.4
0.3
0.2
0.1
0.0
Primary tumor
Metastasis

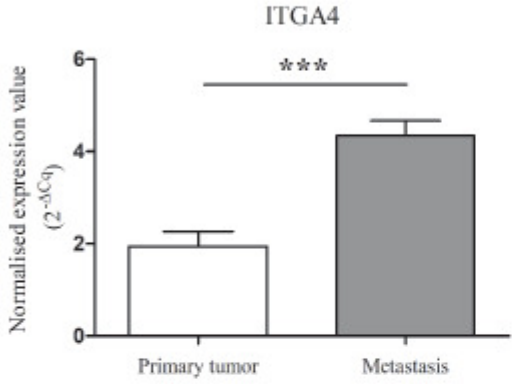
ITGA4
***
Normalised expression value
(2^-ΔCq)
6
4
2
0
Primary tumor
Metastasis

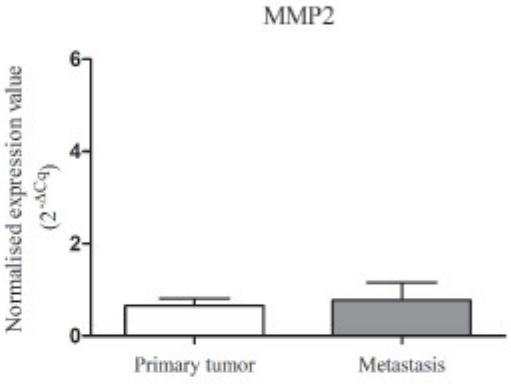
MMP2
Normalised expression value
(2^-ΔCq)
6
4
2
0
Primary tumor
Metastasis

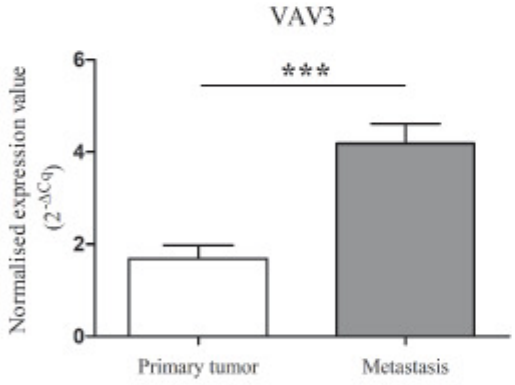
VAV3
***
Normalised expression value
(2^-ΔCq)
6
4
2
0
Primary tumor
Metastasis

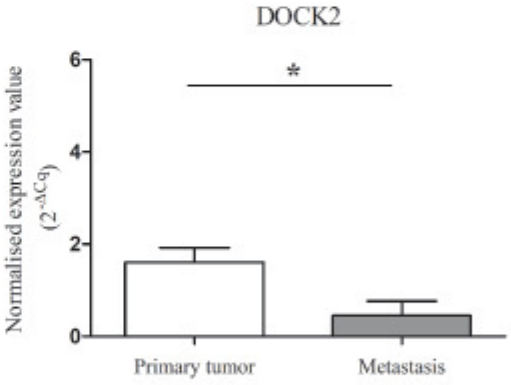
DOCK2
*
Normalised expression value
(2^-ΔCq)
6
4
2
0
Primary tumor
Metastasis

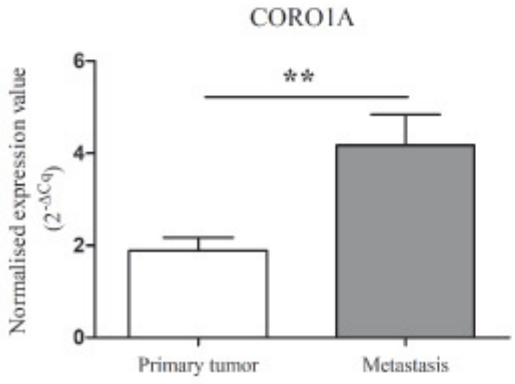
CORO1A
**
Normalised expression value
(2^-ΔCq)
6
4
2
0
Primary tumor
Metastasis

626

Figure 3